JOURNAL OF MATERIALS SCIENCE 29 (1994) 2467–2473

Crystal structure of poly[bis(3,4-dimethylphenoxy)phosphazene]

T. MIYATA, K. YONETAKE, T. MASUKO*
Faculty of Engineering, Yamagata University, Yonezawa 992, Japan

The crystal structure and chain conformation of poly[bis(3,4-dimethylphenoxy)phosphazene] – PB(dMe)PP – have been studied by X-ray diffraction techniques. The unit cell of this polymer shows an orthorhombic form with the crystallographic parameters $a=2.05$, $b=1.49$, c (chain axis) $=0.998$ nm. Its space group is determined as $Pbcn$–D_{2h}^{14} where the molecular chains are located at the centre and each corner of the unit cell, which contains eight monomeric units; these molecular chains possibly have a $-(trans_3cis)_2-$ conformation. The R factor calculated from the final crystal structure was estimated as 16.9%. As with other types of polyorganophosphazenes, the thermotropic transformation in PB(dMe)PP takes place from the three-dimensionally ordered state to its two-dimensional psuedohexagonal form ($a_h=1.49$ nm), accompanied by a latent heat change at 96 °C.

1. Introduction

Due to their side group chemistry, organophosphazene homopolymers are known to have various characteristics, such as excellent mechanical properties, chemical stability, and biocompatibility [1–3]. Interestingly, the first-order thermotropic transitions at a $T(1)$ temperature that appeared in most semicrystalline polyorganophosphazenes (POPs) are influenced by the chemical sizes, polarity and flexibility of the side groups of the polymers [3–7].

It has also been pointed out that polymorphisms of POPs appear after annealing treatment above $T(1)$, depending on the crystallization conditions or the thermal history of the specimens [8–15]. Various structural investigations on these polymers have concentrated on their morphology, crystal modifications and thermal phase transitions [7–25]; however little is known about their exact crystal structures or chain conformations [26–28]. In order to gain better understanding of the crystal/mesomorphic phase transformation from a molecular point of view, the crystal and mesomorphic structures of POPs need to be examined more precisely.

Burkhart *et al.* [28] have proposed by an X-ray diffraction (XRD) technique using oriented specimens that poly[bis(3,4-dimethylphenoxy)phosphazene], PB(dMe)PP, crystal is composed of an orthorhombic lattice with the cell constants of $a = 1.585$, $b = 1.943$, c (chain axis) $= 0.985$ nm. They also suggest that the polymer chains have a $(T_3C)_2$ conformation, where T means *trans* and C *cis*, respectively.

Alternatively, in a previous study [23] we have reported structural features on a solution-grown crystal of PB(dMe)PP, and obtained different lattice constants of the polymer by electron diffraction (ED). In the present work, we further examine the crystal structure of PB(dMe)PP in detail by XRD studies, and also investigate thermal phase transitions of this polymer by means of XRD and differential scanning calorimetry (DSC).

2. Experimental procedure

2.1. Polymer synthesis

Well purified hexachlorocyclotriphosphazene was polymerized in 1,2,4-trichlorobenzene with sulphamic acid to poly(dichlorophosphazene) [29]; the polymer was then reacted with sodium 3,4-dimethylphenoxide in a toluene/diethylene glycol dimethyl ether mixture by use of a well-established procedure [28]. The final product was dissolved in fresh tetrahydrofuran, and then precipitated repeatedly in methanol to obtain the purified polymer, which was white and fibrous in appearance. The elemental analysis and molecular weight obtained by a gel permeation chromatograph are listed in Table I.

2.2. Film specimens

Cast polymer films for XRD measurements were made from a 10 wt % chloroform solution of the polymer on a glass plate in an air oven at 26 °C. Oriented samples were prepared by stretching these films to five times their length at room temperature.

2.3. XRD measurements

Nickel-filtered CuK_α radiation was employed for XRD experiments using a RIGAKU RAD-rA generator operated at 50 kV and 200 mA. XRD photographs for both oriented and unoriented films were taken at room temperature and/or 150 ± 1.0 °C using a heating furnace. Spacings of the reflection phases

* Author to whom all correspondence should be addressed.

TABLE I Characteristics of PB(dMe)PP used in this work

Elemental analysis (%)			IR (cm^{-1})	GPC		
C	H	N		M_n $\times 10^{-4}$	M_w $\times 10^{-4}$	$\bar{M}_w/\bar{M}_n$
66.89	6.31	4.88				
66.00	6.10	4.87	ν P=N 700, 1300 ν P–O–C 1010, 1160	2.41	4.96	2.05

were measured by a flat type camera, correlated with those of $Ca(CO_3)_2$ standard powder. XRD intensity measurements for the oriented film were made using a step-scanning method at a step-width of 0.02° for 20-s intervals in the equatorial direction. The Lorentz polarization factor and multiplicity factor were corrected for observed diffraction intensities. The number of all resolvable reflections reach 23 along the equator line.

2.4. DSC measurements

In order to examine the thermal properties of PB(dMe)PP films, a SEIKO DSC-200 calorimeter was utilized to obtain endothermic and exothermic heat changes in the range of − 50 to 200 °C at heating and cooling rates of 10 °C min^{-1} in a nitrogen atmosphere.

3. Results and discussion

3.1. Lattice dimensions

Fig. 1 shows an X-ray fibre diagram for a PB(dMe)PP-oriented film. All of the reflections in Fig. 1 could be satisfactorily indexed using the orthorhombic lattice constants, $a = 2.05$, $b = 1.49$ and c (chain axis) $= 0.998$ nm, as already reported in a previous study [23]. These constants are different from those reported by Burkhart *et al.* [28]. The fibre repeat distance of 0.998 nm corresponds to the chain length of four monomeric units with a $(T_3C)_2$ conformation, as discussed in detail in a later section. Eight monomeric units are contained in the unit cell, which is determined from the result of density measurement [23].

From the systematic absence of the ED (see Fig. 2 of [23]) and XRD reflections like $hk0$ with $h + k =$ odd, $h00$ with $h =$ odd, $0k0$ with $k =$ odd, $0kl$ with $k =$ odd and $h0l$ with $l =$ odd, the space group $Pbcn$–D_{2h}^{14} could be anticipated as a useful candidate. The eight monomeric units can then be placed in the unit cell, such that the molecular chains pass through the centre and each corner of the unit cell (a, b plane); four monomeric units are involved in the direction of the c-axis (fibre period). These crystal data for this polymer are summarized in Table II.

3.2. Chain conformations and trial packing models

The intensity of reflection is generally expressed by

$$I(hkl) = K m Lp [F(hkl)]^2 \quad (1)$$

where K is a constant, m the multiplicity factor, Lp the Lorentz–polarization factor, and $F(hkl)$ indicates the

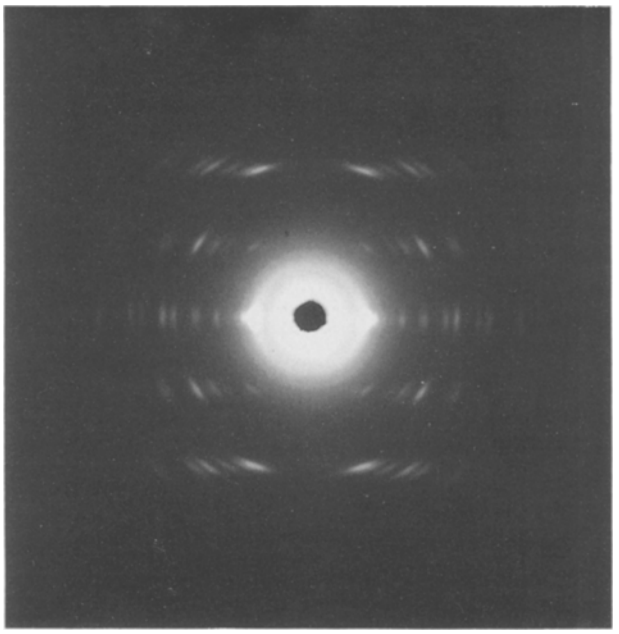

Figure 1 X-ray fibre diagrams for the drawn PB(dMe)PP film.

TABLE II Crystal data of PB(dMe)PP

Crystal system	Orthorhombic
Space group	*Pbcn*
Lattice constants (nm)	
a	2.05
b	1.49
c (f.a.)	0.998
Number of monomeric units per unit cell	8
Number of chains per unit cell	2
Crystal density	
Observed (g/ml)	1.23
Calculated (g/ml)	1.25

structural factor. As the origin of coordinates in this case is taken at the centre of symmetry, the structural factor is expanded as

$$F(hkl) = \sum_s f_s \exp 2\pi i(hx_s + ky_s + lz_s) \quad (2)$$

or

$$F(hkl) = A(hkl) + iB(hkl) \quad (3)$$

$$A(hkl) = \sum_s f_s \cos 2\pi(hx_s + ky_s + lz_s)$$

$$B(hkl) = \sum_s f_s \sin 2\pi(hx_s + ky_s + lz_s)$$

where x_s, y_s, z_s are the three-dimensional fractional coordinates of the sth atom, and f_s its atomic scattering factor (not corrected for thermal vibration in this case). When the space group is to be $Pbcn$–D_{2h}^{14}, the structural factor is then reduced by

$$F(hkl) = \sum_r f_r A_r + i \sum_r f_r B_r \quad (4)$$

where

$$A_r = \cos 2\pi\left(hx_r + \frac{h+k}{4}\right)\cos 2\pi\left(ky_r + \frac{l}{4}\right) \times \cos 2\pi\left(lz_r - \frac{h+k+l}{4}\right)$$

$$B_r = 0$$

The bond length and bond angles utilized in these calculations are shown in Table III. The chain backbone models here are examined by referring to those in polydichlorophosphazene [26].

Studies of conformational analysis for some POPs have been reported by Allen *et al.* [30] using intramolecular non-bonding 6:12 Lennard–Jones and Coulombic potentials. Low potential energy wells are found at the positions which correspond to the approximately *C* and *T* conformations in their report. When we refer to Allen *et al.*'s result, the molecular chains in our case take one of three possible conformations shown in Fig. 2, each of which has different *T* and *C* combinations.

In Fig. 2, model 1 has the $(TC)_4$ planar conformation; model 2 is comprised of the $(T_3C)_2$ geometry. In addition to them, model 3 has the $(T'C'-\bar{T}'\bar{C}')_2$ glide conformation, where the rotation angles are selected as 175° (T') and 30° (C'). This type of the glide model has already been proposed for polydichlorophosphazene chain conformation [26]. These three conformation models composed of four monomeric units can be adjusted to have the same fibre repeat distance as 0.998 nm. Although model 1 is considered to be the most useful chain conformation for several polyphosphazenes [9, 27, 28], this chain model does not satisfy the space group symmetry associated with $Pbcn$–D_{2h}^{14}. Examined in view of the space group symmetry, the molecular chain should have the *c* glide plane conformation along in the perpendicular direction to the *b* axis.

These chain models were packed into the unit cell, as shown in Fig. 3. The temporary structural factors were then calculated. These models were refined by a least-squares method in which a quantity $\sum[(I_o)^{1/2} - (I_c)^{1/2}]$ was minimized using independent, experimental 2 3 reflections, where

$$(I_c)^{1/2} = \left(\sum m F_c^2\right)^{1/2} \quad (5)$$

The notation of F_c in Equation 5 stands for a temporarily calculated structural factor. During the course of refining the model, the existence of hydrogen atoms was not considered. A measure of fits for the model examined was taken in the well-known discrepancy factor *R*, implying

$$R = \frac{|(I_o)^{1/2} - (I_c)^{1/2}|}{(I_o)^{1/2}} \quad (6)$$

The smallest value of *R* was obtained from the crystal structure where the polymer chains with the model 2 conformation were packed into the A-type lattice. This structural model determined involves the $(T_3C)_2$ chain conformation, which can be compared with the result of Burkhart *et al.* [28].

TABLE III Values assumed for bond lengths and bond angles of PB(dMe)PP

Bond length	(nm)	Bond angles	(degrees)
N=P	0.144	N–P–N	115
P–N	0.167	P–N–P	131
P–O	0.157	O–P–O	102
O–C	0.135	P–O–C	120
C–C	0.140	C–C–C	120
C–Me	0.145	C–C–Me	120

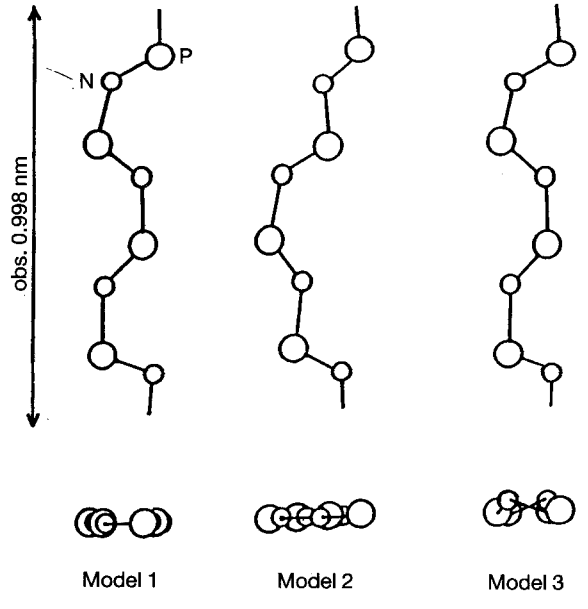

Figure 2 Possible chain conformation models for fitting the observed fibre repeat distance.

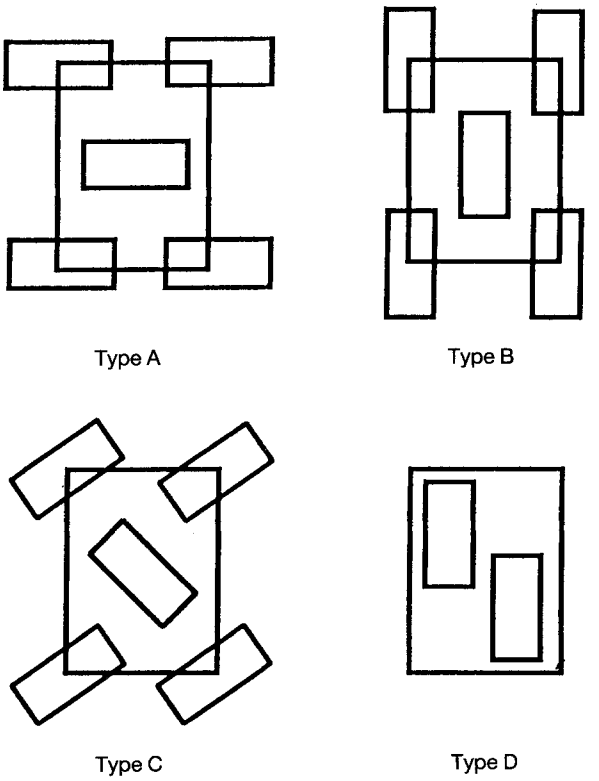

Figure 3 Possible chain packing used in trial model considerations.

3.3. Crystal structure

On reviewing the side-group arrangements, the internal rotation angles made by P–N–O–C_1 bonds and P–O–C_1–C_2 bonds were defined as ψ and ϕ, respectively, as shown in Fig. 4. Some other molecular structure models with different conformation of side groups were also examined. To avoid overlapping van der Waals contacts of hard spheres, trial models were constructed in terms of stereochemical plausibility.

The variation of the R values as a function of the internal rotation angles ϕ is shown in Fig. 5. At the positions of $\phi = 45°$ and 270°, the R value was $< 30\%$; thus several structure models associated with these ϕ values were examined. As a result, the R value at $\phi = 270°$ is smaller than that of the initial trial model, while it remains unchanged at $\phi = 45°$. Therefore the model which has a side-group conformation of $\psi = 45°$ and $\phi = 270°$ was recommended as a reasonable one.

After this refinement, the R value was reduced from 30% for the trial model to 16.9% for the final one. The comparison between observed and calculated structural factors is shown in Fig. 6 using the equatorial reflection. The refined molecular model ('pine cone' model) is schematically illustrated in Fig. 7, and the final chain packing model is shown in Fig. 8. The benzene rings of side groups are flatly stacked in the 'pine cone' chain model. Table IV indicates the list of atomic coordinates for the asymmetric unit in the final model.

The PB(dMe)PP chains located both in the a and b axis directions have the same directional features; however, the alternative configuration of the neighbouring chain appears along the diagonal line. Therefore folding of the molecular chain probably occurs along the $\langle 1\,1\,0 \rangle$ direction. The angle of 72° made by crossing of (1 1 0) and (1 $\bar{1}$ 0) planes is consistent with an acute angle formed by two contour lines, as observed in for PB(dMe)PP solution-grown crystals

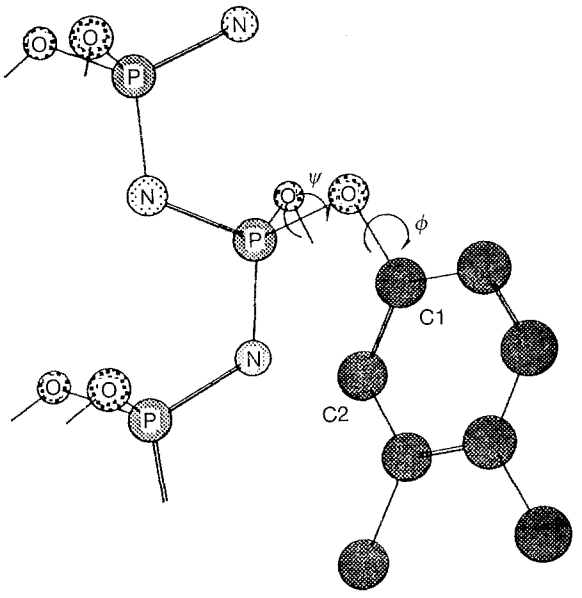

Figure 4 Designation of internal rotation angles in conformation of PB(dMe)PP.

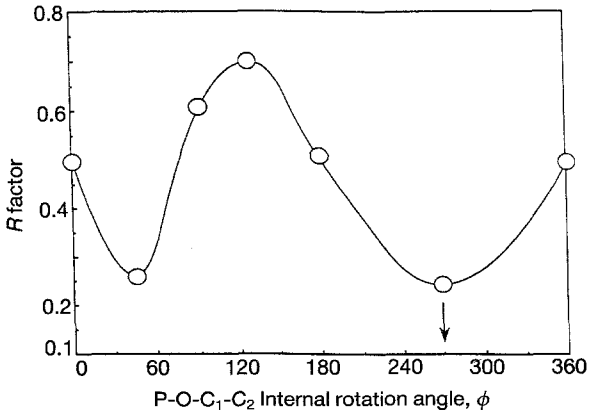

Figure 5 Change in the R value as a function of the internal rotation angle ϕ. $\psi = 45°$.

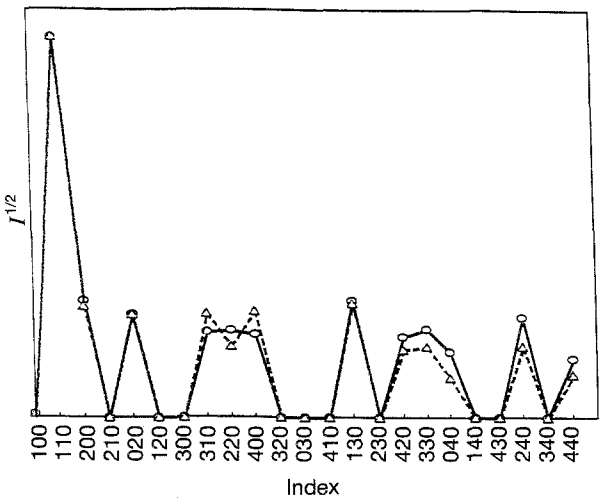

Figure 6 Comparison between the observed (○) and calculated (△) equatorial intensities of PB(dMe)PP.

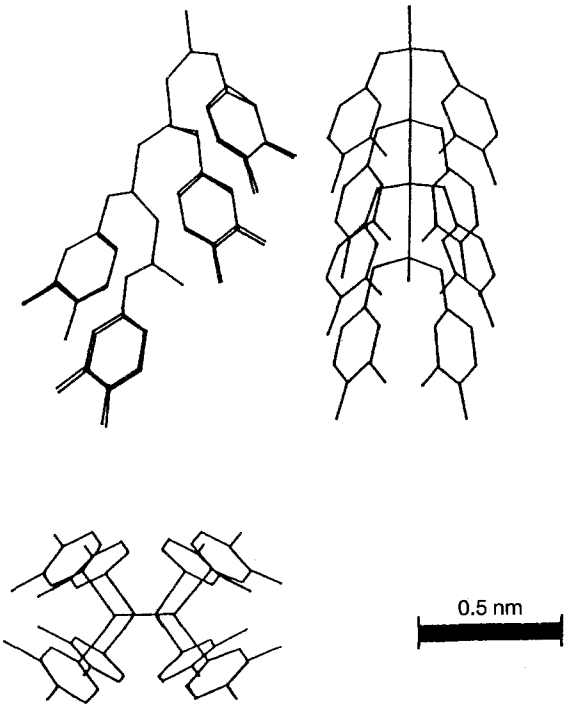

Figure 7 Schematic illustration for the molecular structure of PB(dMe)PP.

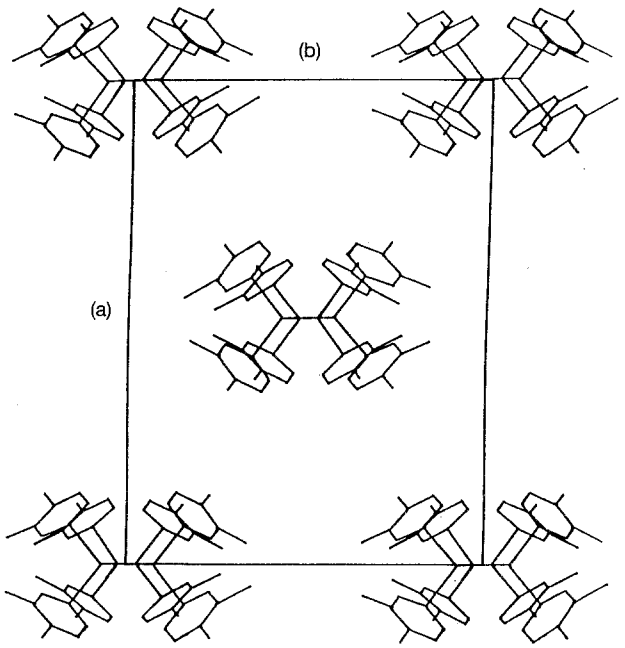

Figure 8 Crystal structure proposed for PB(dMe)PP.

TABLE IV Atomic coordinates of the asymmetric unit

	x	*y*	*z*
P1	0	0.050	0.165
N1	0	0.004	0.275
O1	0.080	0.099	0.183
O2	− 0.083	0.096	0.178
C1	0.111	0.117	0.322
C2	0.073	0.171	0.387
C3	0.101	0.187	0.515
C4	0.167	0.150	0.578
C5	0.206	0.097	0.513
C6	0.178	0.080	0.385
Me1	0.060	0.245	0.586
Me2	0.198	0.168	0.717
C7	− 0.117	0.116	0.315
C8	− 0.186	0.081	0.375
C9	− 0.217	0.099	0.501
C10	− 0.179	0.153	0.566
C11	− 0.109	0.188	0.506
C12	− 0.078	0.169	0.380
Me3	− 0.017	0.245	0.577
Me4	− 0.212	0.173	0.708
P2	0	0.016	0.440
N2	0	− 0.043	0.520
O3	0.085	0.059	0.478
O4	− 0.078	0.061	0.486
C13	0.107	0.071	0.623
C14	0.166	0.030	0.691
C15	0.186	0.042	0.824
C16	0.148	0.095	0.890
C17	0.090	0.137	0.821
C18	0.069	0.125	0.688
Me5	0.049	0.194	0.892
Me6	0.171	0.108	1.030
C19	− 0.095	0.072	0.633
C20	− 0.054	0.125	0.698
C21	− 0.070	0.135	0.833
C22	− 0.127	0.094	0.904
C23	− 0.168	0.042	0.839
C24	− 0.153	0.031	0.703
Me7	− 0.025	0.191	0.904
Me8	− 0.144	0.105	1.050

[23]. Our packing model requires that the setting angle against the (0 1 0) plane is to be zero degrees, in order to satisfy the symmetry of *Pbcn*. As seen in Fig. 5, the value of the *R* factor oscillates depending upon the rotating angle of ϕ. This feature may come from avoiding the space positions of *m*-methyl groups.

Although the crystal structures proposed are different from each other, the value of *R* factor for our structural model and that proposed by the Burkhart model are almost the same. If re-examined with thermal vibration parameters in detail, the *R* value of our model would be improved.

3.4. Thermotropic transition of PB(dMe)PP

Fig. 9 shows the DSC traces of cast PB(dMe)PP film obtained from the heating and cooling processes. The glass transition, T_g, of the polymer is located at − 1.5 °C; a single endothermic peak is observed at 96 °C on the first heating (curve 1). Upon cooling from 200 °C, an exotherm appears at 62 °C (curve 2). When the specimen is subsequently heated, a single exothermic peak at 89 °C, and double endothermic peaks at 86 and 109 °C are observed (curve 3). After the second heating and cooling cycle, no more changes in the DSC traces are observed (curve 4 and 5).

XRD patterns of a PB(dMe)PP cast film at elevated temperatures are shown in Fig. 10. All of the reflections at room temperature, trace (a), could satisfact-

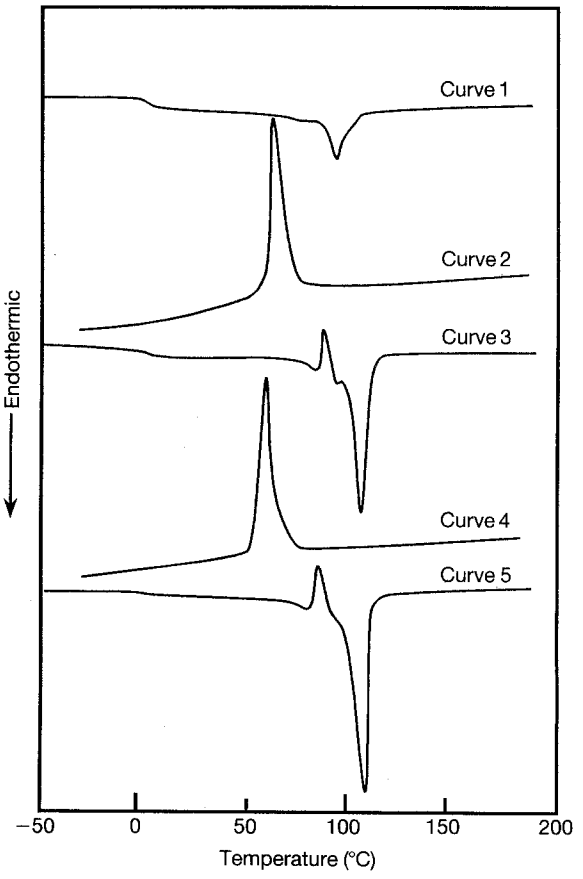

Figure 9 DSC traces of PB(dMe)PP film in various heating/cooling cycles.

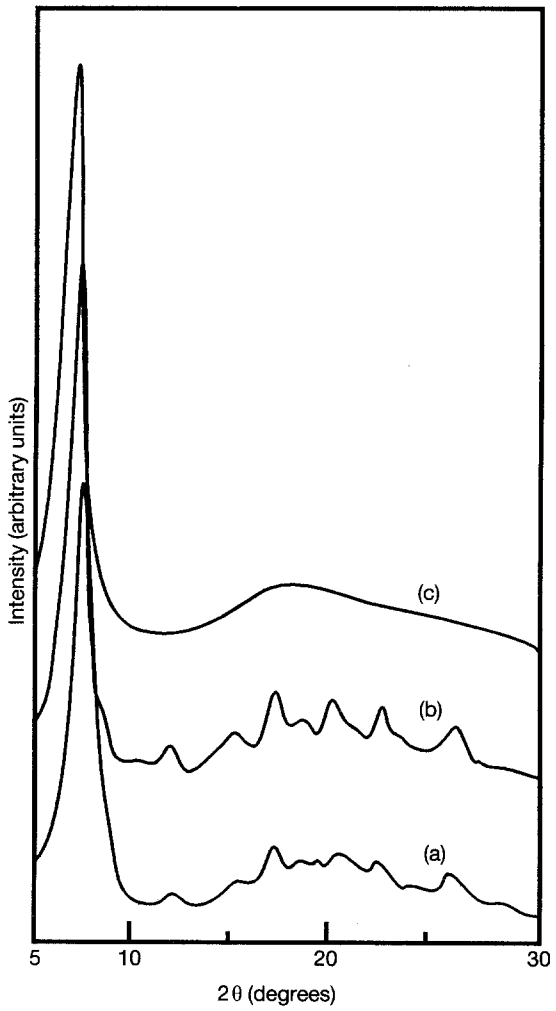

Figure 10 X-ray diffractograms for PB(dMe)PP specimens in various conditions. (a) As-cast film at room temperature; (b) annealed film (200 °C) at room temperature; (c) as-cast film at 150 °C.

orily be indexed using the lattice constants determined. The reflections remain in almost the same positions even at temperatures up to 95 °C (not shown in Fig. 10). At temperatures above the endothermic peak, i.e. 150 °C, trace (c), one strong reflection at $2\theta = 6.85°$ and diffuse halo were observed. These results of XRD and DSC suggest the existence of a mesomorphic phase (δ-form) in the polymer. Therefore the transition located at 96 °C corresponds to the crystal/mesomorphic phase transition, $T(1)$, of PB(dMe)PP.

The distinct reflection in trace (c) at $2\theta = 6.85°$ indicates the existence of intermolecular order, and the halo the absence of well-ordered intramolecular distance. The former is attributed to the 1 0 0 reflection of a pseudohexagonal lattice, and the value of interplanar distance $d(1\,0\,0)_\delta$ is calculated as 1.29 nm. The pseudohexagonal lattice parameter a_h calculated from $d(1\,0\,0)_\delta$ is 1.49 nm, related to the distance among neighbouring chains; Kojima & Magill propose a correlation between the size of side group and lattice parameter in δ-form [5].

The observed narrowing of the ^1H, ^{13}C and ^{31}P lines above $T(1)$ in NMR studies [31–33] suggests that rapid rotational motions of both the side groups and chain backbone occur in the mesomorphic phase for some POPs. The proposed pseudohexagonal lattice has its origin in the virtual cylindrical cross section of the rapidly rotating chains. Fig. 11 shows the δ-form structure model proposed for PB(dMe)PP.

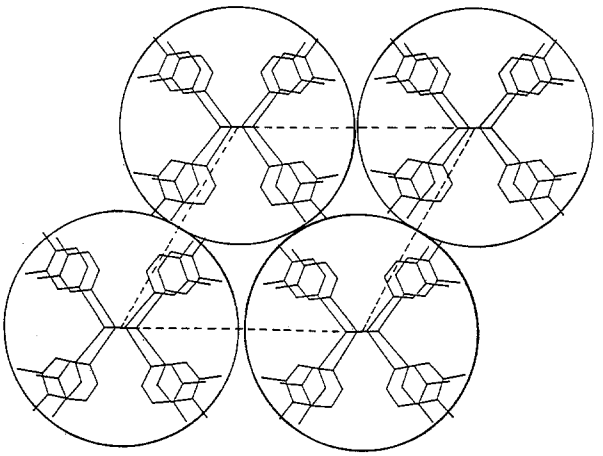

Figure 11 Mesomorphic structure of PB(dMe)PP.

It has been shown that monoclinic lattices of polyphosphazenes transform into orthorhombic forms through the mesomorphic phase in some cases [4]. In Fig. 10, emphasis should be placed on the fact that our XRD results for the sample annealed at 200 °C, far above $T(1)$, show almost similar diffraction patterns to those for as-cast films, trace (b). This suggests that PB(dMe)PP does not involve any crystal modifications. Therefore, the DSC endotherm peak at the lower temperature on second heating probably originates from fusion of smaller crystallites formed by a low molecular weight fraction within the sample.

4. Conclusions

The crystal structure and thermotropic transitions of PB(dMe)PP were investigated using XRD and DSC techniques. The unit cell of this polymer is orthorhombic with the following lattice parameters: $a = 2.05$, $b = 1.49$, and c (chain axis) = 0.998 nm. Molecular chains are placed at the corner and centre of the unit cell, according to the symmetry of the space group $Pbcn$–D_{2h}^{14}. The chain conformation is anticipated to have a $-(trans_3cis)_2-$ sequence. The R factor determined from the final crystal structure was estimated as 16.9%. The PB(dMe)PP crystal transforms to its mesomorphic state of a two-dimensional pseudohexagonal lattice ($a_h = 1.49$ nm) at 96 °C. More detailed structural studies on the thermotropic transitions of this polymer will be reported in the near future.

Acknowledgements

The authors appreciate the contributions of Mr Kazuo Sasaki of Yamagata University, who carried out part of the X-ray work and materials arrangements.

References

1. H. R. ALLCOCK, *Science* **193** (1976) 1214.
2. J. E. MARK, H. R. ALLCOCK and R. WEST, in "Inorganic

Polymers" (Prentice-Hall, Englewood Cliffs, New Jersey, 1992) p. 61.
3. R. E. SINGLER, N. S. SCHNEIDER and G. L. HAGNAUER, *Polym. Eng. Sci.* **15** (1975) 34.
4. R. E. SINGLER, R. A. WILLINGHAM, C. NEAL, C. FRIEDRICH, L. BOSICE and E. D. F. ATKINS, *Macromolecules* **24** (1991) 510.
5. M. KOJIMA and J. H. MAGILL, *Polymer* **30** (1989) 579.
6. M. A. GOMEZ, C. MARCO, J. G. FATOU, T. N. BOWMER, R. C. HADDON and S. V. CHICHESTER-HICKS, *Macromolecules* **24** (1991) 3276.
7. J. H. MAGILL, *J. Inorg. Organometal. Polym.* **2** (1992) 213.
8. M. KOJIMA and J. H. MAGILL, *Makromol. Chem.* **186** (1985) 649.
9. S. V. MEILLE, W. PORZIO, G. ALLEGRA, G. AUDISIO and M. GLERIA, *Makromol. Chem. Rapid Commun.* **7** (1986) 217.
10. S. V. MEILLE, W. PORZIO, A. BOLOGENESI and M. GLERIA, *ibid.* **8** (1987) 43.
11. M. KOJIMA, H. SATAKE, T. MASUKO and J. H. MAGILL, *J. Mater. Sci. Lett.* **6** (1987) 675.
12. M. KOJIMA, T. MASUKO and J. H. MAGILL, *Makromol. Chem. Rapid Commun.* **9** (1988) 565.
13. M. KOJIMA, D. C. SUN and J. H. MAGILL, *Makromol. Chem.* **190** (1989) 1047.
14. M. KOJIMA and J. H. MAGILL, *Polymer* **30** (1989) 1856.
15. T. MIYATA, T. MASUKO, M. KOJIMA and J. H. MAGILL, *Makromol. Chem.*, to appear.
16. C. R. DESPER and N. S. SCHNEIDER, *Macromolecules* **9** (1976) 424.
17. M. N. ALEXANDER, C. R. DESPER, P. L. SAGALYN and N. S. SCHNEIDER, *ibid.* **10** (1977) 721.
18. C. R. DESPER, N. S. SCHNEIDER and E. HIGGINBOTHAM, *J. Polym. Sci., Polym. Lett. Ed.* **15** (1977) 457.
19. M. KOJIMA and J. H. MAGILL, *Polym. Commun.* **24** (1983) 329.
20. M. KOJIMA, W. KLUGE and J. H. MAGILL, *Macromolecules* **17** (1984) 1421.
21. T. MASUKO, M. HOSHI, J. KITAMI and K. YONETAKE, *J. Mater. Sci. Lett.* **7** (1988) 1421.
22. H. HOZUMI, C. KOHAMA, K. YONETAKE and T. MASUKO, *ibid.* **10** (1991) 1187.
23. T. MASUKO, T. MIYATA, H. HOZUMI and K. YONETAKE, *ibid.* **11** (1992) 157.
24. T. MASUKO, R. J. SIMEONE, J. H. MAGILL and PLAZEK, *Macromolecules* **17** (1984) 2857.
25. M. KOJIMA and J. H. MAGILL, *Makromol. Chem.* **193** (1992) 379.
26. Y. CHATANI and K. YATSUYANAGI, *Macromolecules* **20** (1987) 1042.
27. S. H. BISHOP and I. H. HALL, *Br. Polym. J.* **6** (1974) 193.
28. C. W. BURKHART, P. C. GILLETTE, J. B. LANDO and J. J. BERES, *J. Polym. Sci., Polym. Phys. Ed.* **21** (1983) 2349.
29. D. SINCLAIR, US Patent 4242316 (30 December 1980).
30. R. W. ALLEN and H. R. ALLCOCK, *Macromolecules* **9** (1976) 956.
31. H. TANAKA, M. A. GOMEZ, A. E. TONELLI, S. V. CHICHESTER-HICKS and R. C. HADDON, *ibid.* **21** (1988) 2301.
32. H. TANAKA, M. A. GOMEZ, A. E. TONELLI, S. V. CHICHESTER-HICKS and R. C. HADDON, *ibid.* **22** (1989) 1031.
33. S. C. YOUNG and J. H. MAGILL, *ibid.* **22** (1989) 2551.

Received 7 January
and accepted 19 October 1993